Feature Article

Photorefractive Polymer Composites with Short Response Times†

B. Kippelen, E. Hendrickx, K. B. Ferrio, J. Herlocker, Y. Zhang, N. Peyghambarian
Optical Sciences Center, The University of Arizona, Tucson, Arizona

S. R. Marder, J. Anderson, N. R. Armstrong
Department of Chemistry, The University of Arizona, Tucson, Arizona

S. Mery
IPCMS, Groupe des Matériaux Organiques, CNRS, Strasbourg, France

We report on a photorefractive polymer composite that shows an initial rise time of 4 ms at a grating spacing of 3.1 μm. A systematic characterization of the ionization potential of a series of chromophores used in photorefractive applications is presented. No obvious correlation between material response time and ionization potential is found in PVK:ECZ:TNFDM composites doped with chromophores with an ionization potential higher or comparable to that of carbazole. All the chromophores under investigation are found to form a charge-transfer complex with the sensitizer TNFDM and a correlation between the spectral position of this band and the value of the ionization potential of the chromophore is demonstrated.

Journal of Imaging Science and Technology 43: 405–412 (1999)

Introduction

The research on photorefractive polymers is truly interdisciplinary and is at the cross-road of numerous current topics related to basic phenomena such as charge injection and charge transfer in organic amorphous solids. Photorefractive polymers are not only of great academic interest, but with their plasticity and other unique properties, they constitute a strategic class of materials because they enable mass production at low cost of new devices with low weight and high performance. As a reconfigurable recording medium with high dynamic range that is compatible with low power laser diodes or Ti:Sapp lasers, photorefractive polymers are promising for numerous photonic applications including time-average interferometry,[1] optical correlation,[2] and imaging through scattering media using holographic time gating techniques.[3] In addition, the high two-beam coupling gain can be used for optical amplification, self-pumped oscillators,[4] and for optical limiting.[5]

During the past eight years, this new field of research experienced several milestones. A first milestone in this field occurred with the report by the IBM group of net gain and a diffraction efficiency of 1% in 125 μm thick samples of the composite FDEANST:PVK:TNF.[6] Shortly after, we reported on a composite, based on the photoconductor PVK:TNF doped with the chromophore DMNPAA, that exhibited 6% diffraction efficiency in 100 μm thick films.[7] This significant improvement was achieved by adding an additional plasticizer ECZ to the composite. The reduction of the glass transition temperature enabled the orientation of the electrooptic chromophores in the applied field at room temperature. By improving the sample fabrication conditions, higher fields could be applied and nearly 100% diffraction efficiency, net gain coefficients of 200 cm^{-1}, and fully reversible index modulation amplitudes of 0.001 with a response time of 200–500 ms were demonstrated.[8] This high dynamic range was attributed to an orientational birefringence contribution caused by the spatially modulated orientation of the chromophores by the total field in the polymer.[9] The observation of a change in coupling direction when changing the polarization of the beams from *p* to *s* in DMNPAA:PVK:ECZ:TNF samples was clear evidence that the dynamic range was indeed dominated by the orientational birefringence.[8]

The dominant orientational contribution of the overall refractive index modulation amplitude in low *Tg* photorefractive polymers completely changed the selection criteria for chromophores: the Pockels effect was no longer the main driver but rather the birefringence induced by the polarization anisotropy of the dopant chromophore.[9] A new form of photorefractivity was born: orientational photorefractivity where the index of a material is changed through the control of the orientation of anisotropic dopant molecules with a permanent dipole moment by the internal space charge field that is produced, like in a traditional photorefractive material, by absorption, charge separation, and trapping.

Original manuscript received November 12, 1998

† Dedicated to the memory of our collegue, Dr. Paul Borsenberger

Recently, photorefractive polymers with unprecedented high dynamic range were obtained using chromophore design criteria dictated by orientational photorefractivity. However, higher Dn was obtained at the expense of longer response time.[7,10] Similarly, short response times could be obtained in materials with lower Dn.[11] Based on current models for photoconductivity in amorphous organic materials, trapping, or the relative energetical position of the orbitals of the different constituents in the photorefractive composite is expected to influence the response time of a given composite. Similarly, the photoconduction is also expected to be affected by the high dipole moment of the chromophore that is required for high dynamic range according to the design criteria developed for orientational photorefractivity. In this study, we determine the ionization potential or the position of the highest occupied molecular orbital (HOMO) of several photorefractive chromophores and investigate its effect on the photorefractive response time. In particular, we show that the relative position of the HOMO level of the chromophore, with respect to the hole transport moiety, can be deduced from the relative position of the maximum of the absorption of the charge transfer complex formed between the sensitizer and the chromophore and that formed between the sensitizer and the hole transport moiety. We also report on a photorefractive composite with a 4 ms response time.

Theory

Chromophore Design. Like macroscopic systems, molecules exhibit second order nonlinearities only if the centrosymmetry is broken. This can be achieved in conjugated molecules by connecting each end of the conjugated path with groups that have a different electronic affinity. In other words, the symmetry can be broken by deforming the π electron distribution by attaching a donor-like group at one end and an acceptor-like group at the other end. These functional groups are sometimes called moieties or substituents and this class of molecules is referred to as *push–pull* molecules, or chromophores. Due to a difference in charge distribution at the acceptor and donor side, the molecule has a dipole moment in its ground state. The response of the molecule to an electric field, or its polarizability, will strongly depend on the direction of the applied field with respect to the molecule: charge flow is favored towards the acceptor, while hindered towards the donor. This asymmetric polarization permits second-order nonlinear optical properties. The structure of these molecules enables an intramolecular charge transfer via the conjugation path.

When a poling field is applied, orientation of these chromophores leads to macroscopic electrooptic properties but also to birefringence. In the oriented gas model, and for a poling field applied along the Z axis, these two effects can be described[9,12] by:

$$\Delta n_Z^{(1)} = \frac{2\pi}{n} N F^{(1)} \Delta\alpha \, (< \cos^2 \theta > - 1/3) \qquad (1)$$

$$r_{ZZ} = -\frac{8\pi}{n^4} N F^{(2)} \beta < \cos^3 \theta > \qquad (2)$$

where $F^{(1)}$ and $F^{(2)}$ are local field correction factors, $\Delta\alpha$ is the polarizability anisotropy of the chromophore, i.e., the difference between the polarizability along the molecular axis and the polarizability in a perpendicular direction, β the first hyperpolarizability, N the density of molecules, and θ the polar angle between the poling field direction and the dipole moment of the molecule. The averaged quantities $<\cos^n\theta>$ are given by the Langevin functions $L_n(x)$, with $x = \mu E/kT$ where μ is the dipole moment and kT the thermal energy. In the low poling field limit, the Langevin functions can be approximated by $L_2(x) \approx 1/3 + 2x^2/45$, and $L_3(x) \approx x/5$. With these approximations, and from Eqs. 1 and 2, a possible molecular figure of merit for the chromophore for orientational photorefractivity becomes:

$$Q_{OP} = N_{\max} \, (A(T) \, \Delta\alpha \, \mu^2 + \beta\mu) \qquad (3)$$

where $N_{\max}$ is the maximum density of chromophores that can be doped or functionalized in the low glass transition polymer composite before chromophore aggregation or interaction occurs, and $A(T)$ is a scaling factor. The subscript OP in Q_{OP} stands for *orientational photorefractivity*. Note that the first term in the RHS of Eq. 3 scales with the dipole moment squared. This quadratic dependence on dipole moment is due to the Kerr–like character of the orientational birefringence.

Note that all the orientational photorefractive properties are contingent on the ability of the chromophores to orient at the operation temperature—when the temperature is close or above the glass transition temperature T_g. The most efficient polymers to date are based on such orientational photorefractivity. However, polymers with high T_g can be designed where poling (orientation of the chromophores) is achieved at high temperature and frozen in the material, leading to a spatially uniform electrooptic coefficient. In this case, photorefractivity is described by the Pockels effect like in inorganic photorefractive crystals.

A powerful property of organic materials is that the mechanical, optical, and electronic properties can be tuned and optimized using molecular engineering. However, at the same time, that structural flexibility can make chromophore design a very challenging task because optimization of one property should be achieved without compromising another. Thus, systematic structure-property relationships have to be established in order to advance the field of organic photorefractive materials.

One important factor in the design of molecules is the ability to adjust their optical properties. Recently, the BLA (Bond Length Alternation) model[13] was successfully applied to the design of chromophores for photorefractive applications, and the dynamic range could be improved.[3] Within that model, molecular quantities such as dipole moment, polarizability, as well as hyperpolarizability can be correlated with the degree of ground-state polarization. Donor-acceptor substituted molecules with a π-electron conjugation path have a ground-state structure that can be viewed as a linear combination of two limiting resonance forms: a neutral form and a charge-separated form. The relative contribution of these two forms in the ground state can be correlated to the values of BLA or BOA (Bond Order Alternation), where BOA is the difference in the π-bond order between adjacent carbon–carbon bonds. BOA and BLA is usually varied by changing the strength of the donor and acceptor substituents, or by changing the properties of the surrounding medium, such as its polarity. Model calculations[14] showed that chromophores are optimized for BOA values beyond the cyanine limit, where β is roughly maximized in amplitude with a negative sign, in contrast to previous studies that suggested an optimal figure of

merit at the point where β vanishes and when the polarizability anisotropy is maximal.[15] Experimental studies validated the design,[3] however, higher dynamic range was obtained at the expense of longer response time, illustrating the need to comply simultaneously with other requirements influencing transport and photogeneration efficiency, as discussed previously.

Photogeneration

Photogeneration can be divided in two steps: the electron-hole generation process followed by a charge transfer between the sensitizer and the transport molecule. The creation of a correlated electron-hole pair (or exciton) after absorption of a photon can be followed by recombination. This process limits the formation of free carriers that participate in the transport process and is therefore a loss for the formation of the space-charge unless an electric field is applied to counteract recombination. The quantum efficiency for carrier generation is therefore strongly field-dependent and increases with the applied field.

In other words, photogeneration is governed by an electron transfer reaction between the sensitizer and transport molecules. As known from the Marcus theory,[16] rate constants for this reaction are expected to depend not only on the molecular size and shape of molecules, but also on the properties of the surrounding matrix, in particular its polarity.

The quantum efficiency for carrier generation is therefore strongly field dependent and increases with the applied field. A theory developed by Onsager[17] for the dissociation of ion pairs in weak electrolytes under an applied field has been found to describe reasonably well, the temperature and field dependence of the photogeneration efficiency in some of the organic photoconductors. A good numerical approximation to Onsager's quantum efficiency $\phi(E)$ was given by Mozumder[18] in terms of the infinite sum:

$$\phi(E) = \phi_0 \left[1 - \zeta^{-1} \sum_{n=0}^{\infty} A_n(\kappa) A_n(\zeta) \right] \tag{4}$$

where $A_n(x)$ is a recursive formula given by:

$$A_n(x) = A_{n-1}(x) - \frac{x^n \exp(-x)}{n!}, A_0(x) = 1 - \exp(-x). \tag{5}$$

In Eq. 4, ϕ_0 is the primary quantum yield, i.e., the fraction of absorbed photons that results in bound thermalized electron-hole pairs. It is considered independent of the applied field. $\kappa = r_c / r_0$ and $\zeta = e\, r_0\, E \,/\, k_B T$ where $r_c = e^2/\varepsilon\, kT$, and e is the elementary charge, ε_0 the permittivity, ε the dielectric constant, kT is the thermal energy, and r_0 is a parameter that describes the thermalization length between the bound electron and hole.

Transport

After photogeneration of free carriers, the next step in the buildup of a space-charge is their transport from brighter regions of the interference pattern, where they are generated to the darker regions where they get trapped. In contrast to inorganic photorefractive crystals with a periodic structure, photorefractive polymers have a nearly amorphous structure. The local energy level of each molecule/moiety is affected by its nonuniform environment. As a result, transport can no longer be described by band models, but is attributed to hopping of carriers between neighboring molecules or moieties.

In recent years, a model[19] based on disorder due to Bässler and Borsenberger describes the transport phenomena in a wide range of different materials and emerged as a solid formalism to describe the transport in amorphous organic materials. This so-called disorder formalism is based on the assumption that charge transport occurs by hopping through a distribution of localized states with energetical and positional disorder. So far, most of the predictions of this theory agree reasonably well with the experiments performed in a wide range of doped polymers, main-chain and side-chain polymers and in molecular glasses.[20–25]

In the Bässler formalism, disorder is separated into diagonal and off-diagonal components. Diagonal disorder is characterized by the standard deviation σ of the Gaussian energy distribution of the hopping site manifold (energetical disorder) and the off-diagonal component is described by the parameter Σ that describes the amount of positional disorder. Results of Monte-Carlo simulations led to the following universal law for the mobility:

$$\mu_t(E,T) = \mu_0 \exp\left[-\left(\frac{2\sigma}{3kT} \right)^2 \right] \exp\left\{ C \left[\left(\frac{\sigma}{kT} \right)^2 - \Sigma^2 \right] E^{1/2} \right\} \tag{6}$$

where μ_0 is a mobility prefactor and C an empirical constant. Equation 6 is valid for high electric fields (a few tens of V/μm) and for temperatures $T_g > T > T_c$ where T_g is the glass transition temperature and T_c the dispersive to nondispersive transition temperature.

Certain conclusions can be drawn from Eq. 6, (i) the mobility is strongly field and temperature dependent, and (ii) the highest mobility values are obtained for the smallest values of the width σ of the density of states. The validity of the Bässler formalism has been extensively tested through numerous experimental studies in neat films of organic transport molecules and in various guest/host systems using the time-of-flight technique. Good agreement was found in most cases. In early studies on guest/host systems, it was generally accepted that the polymer host was inert and played no role in the charge transport. Later, simulations and experimental work showed that the width of the density of states σ was strongly dependent on the polarity of the polymer host and the dipole moment of the dopant molecule. It was found that the total width σ was comprised of a dipolar component σ_D and an independent Van der Waals component σ_{VdW} : [26]

$$\sigma^2 = \sigma_{WdW}^2 + \sigma_D^2 \tag{7}$$

Equations 6 and 7 illustrate that the dipole moment of the dopant chromophore is expected to highly influence the transport properties of the overall photorefractive composite.

Another important parameter that affects hole transport in guest/host systems is the relative position of the HOMO energy level of the different dopant moieties or their ionization potential I_p. Dopant molecules with a lower I_p will act as shallow traps. The trapping depth may not affect only the value of the mobility but also the mobility dependence on trap concentration as was shown in some of Borsenberger's last work.[27]

Orientational Dynamics

In orientational photorefractivity, the response time of hologram formation is not only influenced by the buildup dynamics of the space-charge but also by the orientation dynamics of the chromophores under the total field, that is the superposition of the space-charge field and the applied field. Dynamics of the Kerr birefringence has been studied extensively in the past[28] and is characterized by an orientational factor $\Theta(t)$ which is proportional to the ensemble average of the Legendre polynomials of degree 2 with an angular distribution function given by the rotational diffusion equation. The dynamics of the buildup and the decay of the birefringence can be obtained by solving the rotational diffusion equation.[29] When the chromophores are treated as noninteracting rigid particles with cylindrical symmetry, the buildup process of the birefringence is given by:

$$\Delta n_{BR}^{Bu}(t) / \Delta n_{BR}^{Bu}(\infty) = 1 - B\exp(-2Dt) + (B-1)\exp(-6Dt) \quad (8)$$

where D is the rotational diffusion constant about the transverse axis of the chromophore. In real solid polymer composites, Eq. 8 is not satisfied because the disorder and the coupling of the chromophore with the matrix leads to a distribution of relaxation times. Dielectric relaxation in polymers, as well as poling relaxation experiments in electrooptic polymers, show that the dynamics can be fitted using a stretched exponential (Kohlrausch–Williams–Watts) function $y = C\exp[-(t/\tau)\beta]$ where $\beta < 1$ is a measure of how many relaxation processes are contributing to the process. An alternative, is to use a sum of two exponential functions with two uncorrelated time constants τ_1 and τ_2.

Experimental Procedures

Sample Preparation and Wave–Mixing Experiments. Polymer composites were produced in a conventional matrix of poly–N–vinylcarbazole (PVK), N-ethylcarbazole (ECZ), and (2,4,7-trinitro-9-fluorenylidene) malonodinitrile (TNFDM) with different chromophores. Samples were prepared by laminating a 105 μm thick layer of composite materials between glass slides coated with indium tin oxide (ITO) transparent electrodes. For the four-wave mixing and two-beam coupling measurements, 633 nm writing beams were incident on the sample with an interbeam angle of 20.5° in air outside the sample. The sample surface normal was tilted 60° relative to the writing beam bisector. For samples based on the chromophore FTCN (see Table I), the resulting grating period was 3.1 μm. Electric field bias was applied via the ITO electrodes on the sample. In four-wave mixing experiments, s-polarized writing beams had equal irradiances of 0.25 W/cm^2 in the composite film; a relatively weak p-polarized probe beam counterpropagated with respect to one of the writing beam paths. In two-beam coupling experiments, p-polarized writing beams provided a total sample irradiance of 0.50 W/cm^2 with a beam power ratio of 6.3:1.

Transient Ellipsometry

To compare the transient response of the birefringence to the photorefractive response time, an extension of earlier steady-state ellipsometric techniques[30] was used to measure the transient orientational response of the chromophore. The birefringence induced by a 600 V electric field step was probed with a 690 nm laser diode beam incident at 45° in a polarizer-analyzer configuration.

Photoconductivity Measurements

The photoconductivity and photogeneration efficiency were measured using a typical "time-of-flight" experimental setup. In this experiment a polymer sample of about 105 μm was sandwiched between two glass slides coated with transparent electrodes. The sample was connected electrically in series with a variable resistor. A field was applied to the resulting RC circuit, and the voltage across the resistor was monitored using a digitizing oscilloscope. Any change in the sample's conductivity resulting from illumination could be measured as a change in voltage.

A pulsed laser diode, operating at 830 nm with a 100 ms pulse width, was fed through a multimode fiber (D = 60 μm) that was butt-coupled to the sample. The peak power illuminating the sample was measured to be 36 mW and the spot size was 0.5 cm. The diode was allowed to pulse repeatedly and the average photovoltage was collected on the scope.

The photovoltage V_{ph} was measured as the difference between the plateau region of the measured voltage and the measured dark voltage. The long pulse width insured that quasi-steady-state conditions could be assumed. In this case the conductivity is calculated as:

$$\sigma = \frac{V_{ph}}{RE(\pi r)^2} \quad (9)$$

where R is the resistance, E is the applied field, and r is the spot radius. It is also assumed that the carrier lifetime is long enough so that all of the photogenerated carriers contribute to the measured photocurrent and that the lifetime can be approximated to the transit time of the carrier through the sample. In this case the quantum efficiency can be expressed as:

$$\phi = \sigma \frac{hcE}{\lambda e \alpha d I} \quad (10)$$

where α is the absorption coefficient, d is the thickness of the polymer film and I is the illumination intensity.

Electrochemistry

To estimate the relative positions of the ionization potentials of a series of photorefractive dyes, we used both cyclic voltammetry and optical spectroscopy. Charge transfer complexes are formed between an electron rich molecule (donor) and an electron deficient molecule (acceptor). The complexation leads to the appearance of a new absorption band in the UV/NIR spectrum. A typical example of charge-transfer (CT) complexation is the complex formed between 9-ethylcarbazole (ECZ) and (2,4,7-trinitro-9-fluorenylidene) malonodinitrile (TNFDM), which shows an absorption maximum at 590 nm in acetone solution. Upon photoexcitation of the complex, an electron is transferred from the donor to the acceptor. Electron transfer in complexes have been used extensively in photosensitizers.

It has been shown that, for a given electron acceptor, the position of the charge transfer band correlates with the ionization potential of the electron donor, shifting to lower energies for electron donors with smaller ionization potentials:[31]

$$\hbar\omega_{CT} = a\, I_p + b \qquad (11)$$

where a and b are constants for a given acceptor.

The structures of the photorefractive dyes that were investigated are shown in Table I. Even though most of the dyes have both an electron donor and acceptor group, they were still able to form a complex with TNFDM. Absorption spectra were recorded in acetone of TNFDM alone, dyes alone, and TNFDM + dye. The dye and TNFDM concentrations were in the range from 0.038 to 0.0056 M and 0.069 to 0.0053 M, respectively. The spectrum of the individual components in acetone was then substracted from the absorption spectrum of the mixture. The optical density at the CT-maximum was between 0.3 and 1.3. For a number of dyes, a complexation could be observed, but the maximum coincided with strong absorption from TNFDM or the dye. For dyes 7 and 8, the position of the maximum of the complexation peak was estimated by fitting the observable part of the complexation band to a Gaussian. For dyes 6 and 10, only the onset of the complexation band was observed and an accurate fit could not be obtained.

Cyclic voltammetry was used as a second technique to estimate the relative position of the ionization potentials. Voltammograms were recorded of solutions of dyes in acetonitrile/benzene (1/1) mixture dried over freshly activated alumina. Argon or nitrogen blown through acetonitrile solution over activated alumina were used as purge gas. Tetrabutylammonium hexafluorophosphate (Fluka, electrochemical grade) or tetrabutylammonium perchlorate (recrystallized in ethanol) were used as the supporting electrolyte. The scan rate was 500 mV/s and the curves were referenced to the normal hydrogen electrode (NHE) using ferrocene (E^0 = 0.690 V versus NHE).[32] Because the majority of the dyes the oxidation are nonreversible, we use the onset of the oxidation wave as an estimate of the redox potential. From the redox potential E^0 versus NHE, the ionization potential can be estimated as:[33]

$$I_P\,(eV) = E^0\,(V) + 4.5 \qquad (12)$$

Results and Discussion

The spectral position of the complexation band formed between TNFDM and several photorefractive chromophores is summarized in Table I together with the results of cyclic voltammetry. For carbazole, we measured a corresponding oxidation onset of 1.3 V and $\hbar\omega_{CT}$ = 20.4 eV. As shown in Fig. 1, a good linear correlation could be found between the energy of the CT band and the ionization potential as measured by cyclic voltammetry. Thus, when chromophores 1 to 5 are combined with TNFDM, an absorption band appears with a maximum that is red-shifted compared with the carbazole:TNFDM one. Due to the large width of these bands, in some photorefractive composites these two different absorption bands can overlap at the operating wavelength, precluding a selective excitation of the carbazole:TNFDM complex. In some composites, the excitation in the absorption band caused by the complexation of the chromophore and the sensitizer TNFDM, was leading to some permanent grating formation. As expected, the position of the I_p mainly depends on the nature of the electron donor. Most of the chromophores with an amino donor have an I_p smaller than that of carbazole. Note that when replacing TNFDM with a less deficient electron acceptor such as TNF, the complexation bands formed by carbazole:TNF,

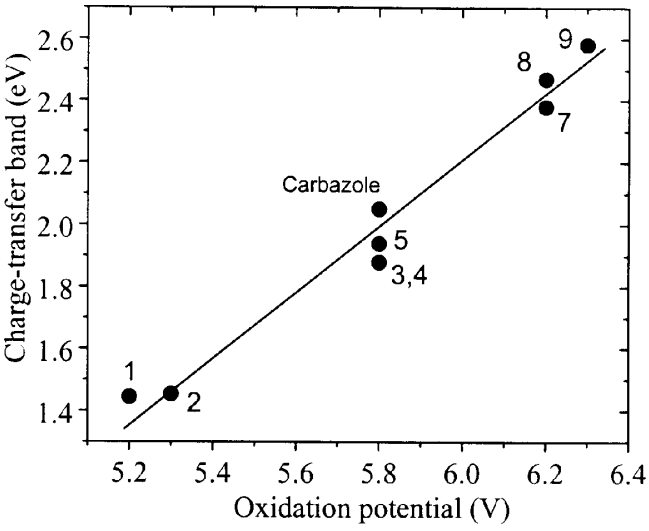

Figure 1. Photon energy of the charge-transfer absorption band between TNFDM and different chromophores versus the ionization potential of the chromophore as measured by cyclic voltammetry. The solid line is a guide to the eye.

and chromophore:TNF, respectively, shift by approximately the same amount, such that selective excitation still does not occur. Comparing chromophores 5 and 6 shows that perfluorination of styrene chromophores can be used to increase the value of the I_p by 0.3 eV. Table I also shows that all the chromophores with an alkoxy donor have I_p values higher than that of carbazole.

To characterize the hologram formation dynamics, we measured the transient diffracted signal in a four-wave mixing experiment. This signal was digitized during the following sequence. Electric field and a single writing beam were applied for several minutes; the second write beam was then switched on to start grating formation. This was done in a sample of FTCN:PVK:ECZ:TNFDM with composition (15.2:56:28:0.8 wt. %) and by varying the electric field from 0 to 95 V/μm. FTCN is the chromophore 9 in Table I. As shown in Fig. 2, the grating buildup can be fitted using a biexponential function of the form:

$$\eta(t) = A\,[\,1 - a\exp(-t/\tau_1) + (a-1)\exp(-t/\tau_2)\,]^2 \qquad (13)$$

where A is the steady-state diffraction efficiency. The best fit to the experimental data was obtained with a = 0.89 and τ_1 = 0.004 s and τ_2 = 0.125 s. The dominant rise time constant of 4 ms is comparable to the fastest response time constant reported so far in a photorefractive polymer[11] consisting of a PVK matrix using butyl benzyl phthalate as a plasticizer, C_{60} as a sensitizer, and the chromophore 7-DCST, corresponding to chromophore 4 in Table I. Prior to this report, the fastest photorefractive polymer was based on a poly(silane) matrix and had a response time of 40 ms but low dynamic range.[34] Recently, photorefractive polymers based on tetraphenyldiaminobiphenyl units showed a response time of 7.5 ms.[11b] Efficient polymers based on DMNPAA:PVK:ECZ:TNF showed response times ranging between 200 ms and tens of s depending on the glass transition temperature T_g.[35] The speed of PVK-based polymers doped with chromophores 4 or 9 is, therefore, significantly higher than that of previously known organic photorefractive materials based on PVK.

TABLE I. Chemical Structure and Numbering Scheme of Several Photorefractive Chromophores—Oxidation Onset and Spectral Position of the Complexation Band Formed with TNFDM

Molecule		Oxidation Onset (V vs NHE)	$\hbar\omega_{CT}$ (eV)
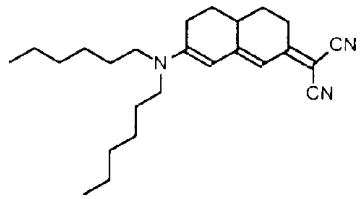	1	0.7	Max : 1.44
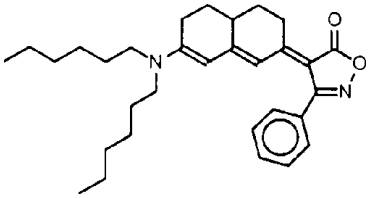	2	0.8	Max : 1.45
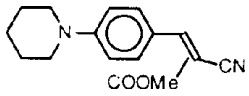	3	1.3	Max : 1.88
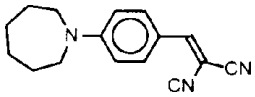	4	1.3	Max : 1.88
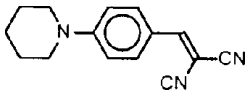	5	1.3	Max : 1.94
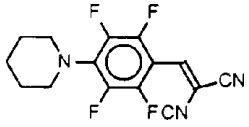	6	1.6	Max: > 2.5 Onset : 2.5
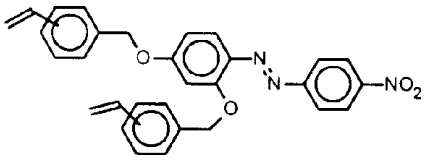	7	1.7	Max: 2.38 (extrapolated) Onset : 1.9
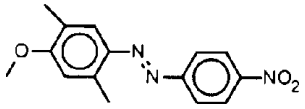	8	1.7	Max: 2.47 (extrapolated) Onset : 1.9
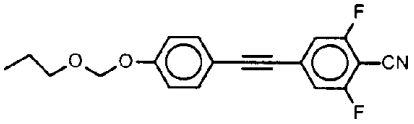	9	1.8	Max : 2.58 Onset : 2.1
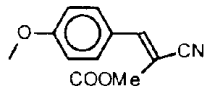	10	1.8	Max > 2.5

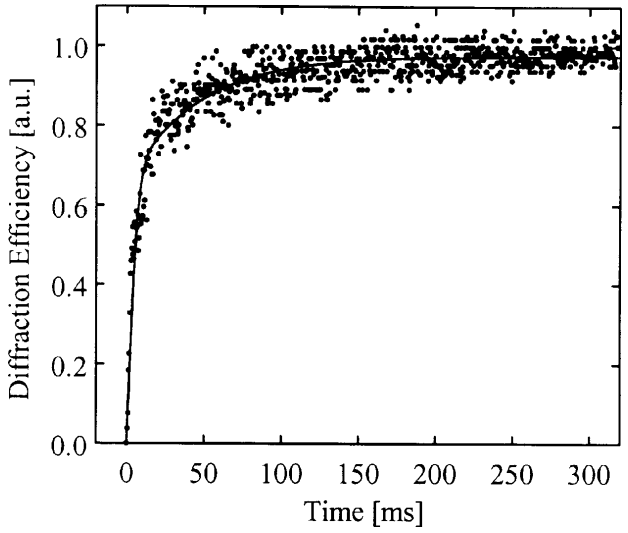

Figure 2. Transient diffracted signal measured in FTCN:PVK:ECZ:TNFDM sample with composition (15.2:56:28:0.8 wt. %) at 95 V/μm and total writing irradiance at the sample of 0.5 W/cm^2.

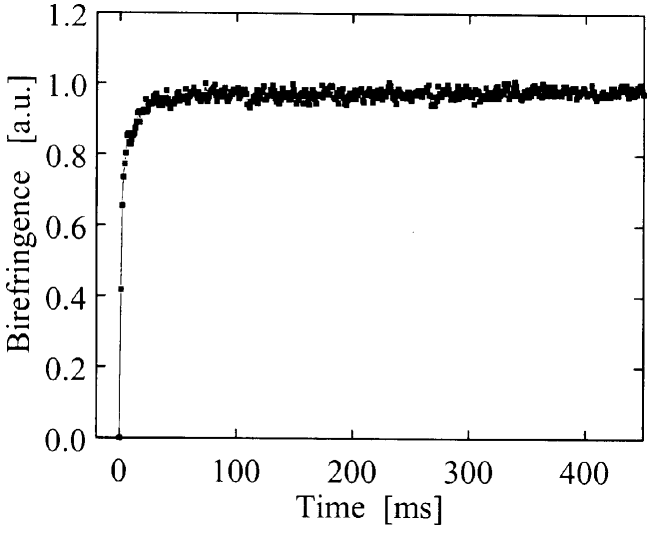

Figure 3. Initial time response of the birefringence measured by transient ellipsometry in the composite FTCN:PVK:ECZ:TNFDM (15.2:56:28:0.8 wt. %).

To determine the limiting factor of the response time of the fast composite FTCN:PVK:ECZ:TNFDM, we carried out a series of characterization experiments. The T_g of the composite did occur over a broad temperature interval of 75°C with an inflection point in the heat capacity at 39°C, as determined by a TA Instruments DSC 2920 modulated differential scanning calorimeter. This indicates that fast response can be obtained when the operation temperature is lower than T_g and is in contrast with what was reported in PVK-based materials doped with DMNPAA (chromophore 8 in Table I) where a response time below 1 s was observed only for composites at temperatures above T_g.[35] In the latter materials, orientational dynamics was found to be the limiting factor when above T_g. To investigate the limiting factor in a composite doped with chromophore 9, we performed transient ellipsometry experiments. The transient field-induced birefringence exhibits several time scales, including an initial rise time τ_1 = 490 μs (see Fig. 3).

Although, chromophores 4 and 9 both lead to materials with short response time in a PVK-based matrix, they have several differences. First, chromophore 9 exhibits good orientational mobility, even though its diphenyl-tolane structure makes its longer than 4. This shows that small size chromophores are not necessarily a requirement for short response time. Second, the ionization potential of the two dyes differs by 0.5 eV as shown in Table I. While the I_p of 4 is almost lined up with that of carbazole (within the sensitivity range of our experiment of ± 0.1 eV), chromophore 9 has a higher I_p and should, therefore, not act as a trap for the carbazole moieties. Chromophore 5, which has an I_p comparable to that of 4, however, did show significantly longer response time. Similarly, 8 and 9 have both a higher ionization potential than carbazole, but lead to materials with different response times.

To investigate the role of the chromophore on the photoconducting properties of the composite, we carried out photoconductivity experiments in the following two samples: PVK:ECZ:TNFDM (61.5:38:0.5 wt. %) and FTCN:PVK:ECZ:TNFDM (15:55:29:0.8 wt. %), referred to as composite A and B, respectively. Following the experimental procedure discussed above, we obtained at

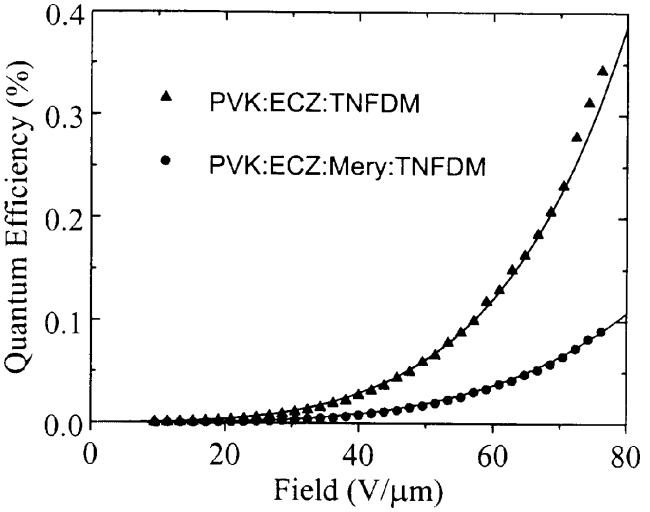

Figure 4. Quantum efficiency derived from the photoconductivity using Eq. 10 as a function of applied field in the composites PVK:ECZ:TNFDM (61.5:38:0.5 wt. %) (triangles) and FTCN:PVK:ECZ:TNFDM (15:55:29:0.8 wt. %) (circles). Solid lines are calculated curves according to Onsager's theory (see text for details).

an applied field of 50 V/μm a photoconductivity value of $\sigma/I = 6.5 \times 10^{-11}$ cm/ΩW for composite A that did not contain any chromophore, and $\sigma/I = 4 \times 10^{-11}$ cm/ΩW for composite B with chromophore. These results show that the presence of a dipolar molecule in the mixture reduces the photoconductivity of PVK-based photoconductors. The corresponding photogeneration efficiency values for both composites are shown in Fig. 4 together with theoretical fits using Onsager's theory and Eq. 4. Note that Eq. 10 is generally a good approximation when the sample is highly absorbing so that most of the carriers are generated near one of the two electrodes. In our case, the samples have a moderate absorption at the wavelength of the experiments. Thus, the absolute values of the photogeneration efficiency might differ by a factor of two from the values derived using Eq. 10. The main point of this study is to compare the relative photogeneration

efficiency of different samples under similar experimental conditions. At the highest field values of 76 V/μm, the photogeneration efficiency in composite A is $\Phi = 0.34\%$, while the one in composite B is only $\Phi = 0.09\%$. For both composites, a good fit could be obtained using Onsager's theory. The parameters used for the fits were $T = 295$ K, and $\varepsilon = 2.75$, $r_0 = 1.455$ nm, $\Phi_0 = 1$ for composite A, and $\varepsilon = 3.0$, $r_0 = 1.25$ nm, $\Phi_0 = 1$ for composite B.

Conclusions

We were able to develop a new photorefractive composite based on the optically transparent FTCN chromophore 9 that showed a response time of 4 ms comparable to 7-DCST, a considerable improvement over previous PVK-based materials doped with DMNPAA or DHADCMPN. To study the influence of the relative value of the ionization potential of the chromophore with respect to the hole transport moiety on the response time of the photorefractive grating formation, we characterized the ionization potential (I_p) of a series of photorefractive chromophores. FTCN 9 was found to have one of the highest I_p and DHADCMPN 1 had the lowest with respect to carbazole. In contrast, chromophore 4 that has been used previously in photorefractive composites[11] with short response time and has an I_p that is almost lined up with that of carbazole (within the sensitivity range of our experiment of ± 0.1 eV). At this stage, several conclusions can be drawn from our studies:

(i) the design of a chromophore with an I_p comparable or higher than that of the transport moiety does not necessarily guarantee short response time;
(ii) chromophores with a length larger than that of DMNPAA 8 can have a fast orientational mobility;
(iii) while in some composites (e.g., DMNPAA) the photorefractive response time is limited by orientational mobility of the chromophore,[35] in PVK composites doped with FTCN the photoconductivity is found to be the limiting factor like in materials doped with 7-DCST;
(iv) the photoconductivity and photogeneration efficiency of the transport matrix is significantly reduced by the chromophore. This study also showed that all the chromophores under investigation do form a charge-transfer complex with the sensitizer TNFDM and that the spectral position of the band is correlated to the ionization potential of the chromophore.

Further studies are being conducted to determine if the long response-time of DHADCMPN-based material is caused by low carrier-mobility. The large dipolemoment of the chromophore may impair the carrier-mobility by broadening the density of states, in agreeement with the work by Borsenberger in organic photoconductors. Other possible explanations, such as orientational mobility and photogeneration efficiency are also being investigated.

Acknowledgments. This work was supported by AFOSR, ONR through the MURI Center for Advanced Multifunctional Nonlinear Optical Polymers and Molecular Assemblies, NSF, an international NSF/CNRS collaboration, and a NATO Travel Grant. E. H. is a postdoctoral research assistant of the Fund for Scientific Research–Flanders (Belgium).

References

1. B. L. Volodin, Sandalphon, K. Meerholz, B. Kippelen, N. Kukhtarev, and N. Peyghambarian, *Opt. Eng.* **34,** 2213 (1995).
2. B. L. Volodin, B. Kippelen, K. Meerholz, B. Javidi, and N. Peyghambarian, *Nature* **383,** 58 (1996).
3. B. Kippelen, S. R. Marder, E. Hendrickx, J. L. Maldonado, G. Guillemet, B. L. Volodin, D. D. Steele, Y. Enami, Sandalphon, Y. J. Yao, J. F. Wang, H. R. Röckel, L. Erskine, and N. Peyghambarian, *Science* **279,** 54 (1998).
4. Grunnet-Jepsen, C. L. Thompson and W. E. Moerner, *Science* **277,** 549 (1997).
5. Grunnet-Jepsen, C. L. Thompson, R. J. Twieg, and W. E. Moerner, *J. Opt. Soc. Am. B* **15,** 901 (1998).
6. M. C. J. M. Donckers, S. M. Silence, C. A. Walsh, F. Hache, D. M. Burland, and W. E. Moerner, *Opt. Lett.* **18,** 1044 (1993).
7. B. Kippelen, Sandalphon, N. Peyghambarian, S. R. Lyon, A. B. Padias, and H. K. Hall Jr., *Electron. Lett.* **29,** 1873 (1993).
8. K. Meerholz, B. L. Volodin, Sandalphon, B. Kippelen, and N. Peyghambarian, *Nature* **371,** 497 (1994).
9. W. E. Moerner, S. M. Silence, F. Hache, and G. C. Bjorklund, *J. Opt. Soc. Am. B* **11,** 320 (1994).
10. E. Hendrickx, B. L. Volodin, D. D. Steele, J. L. Maldonado, J. F. Wang, B. Kippelen, and N. Peyghambarian, *Appl. Phys. Lett.* **71,** 1159 (1997).
11. D. Wright, M.A. Díaz-García, J. D. Casperson, M. DeClue, W. E. Moerner, and R.J. Twieg, *Appl. Phys. Lett.* **73,** 1490 (1998); K. Ogino, T. Nomura, T. Shichi, S.-H. Park, H. Sato, T. Aoyama, and T. Wada, *Chem. Mater.* **9,** 2768 (1997).
12. B. Kippelen, K. Meerholz and N. Peyghambarian, in *Nonlinear Optics of Organic Molecules and Polymers*, H. S. Nalwa and S. Miyata, Eds., CRS, Boca Raton, 1997, p. 465.
13. S. R. Marder, D. N. Beratan and L.-T. Cheng, *Science* **252,** 103–106 (1991).
14. B. Kippelen, F. Meyers, N. Peyghambarian, and S. R. Marder, *J. Am. Chem. Soc.* **119,** 4559 (1997).
15. R. Wortmann, C. Poga, R. J. Twieg, C. Geletneky, C. R. Moylan, P. M. Lundquist, R. G. DeVoe, P. M. Cotts, H. Horn, J. E. Rice, and D. M. Burland, *J. Chem. Phys.* **105,** 10637 (1996).
16. R. A. Marcus and N. Sutin, *Biochimica et Biophysica Acta* **811,** 265 (1985).
17. L. Onsager, *Phys. Rev.* **54,** 554 (1938).
18. M. Mozumder, *J. Chem. Phys.* **60,** 4300 (1974).
19. H. Bässler, *Adv. Mat.* **5,** 662 (1993).
20. P. M. Borsenberger and D. S. Weiss, *Organic photoreceptors for imaging systems*, Marcel Dekker, Inc., New York, 1993.
21. P. M. Borsenberger, *J. Appl. Phys.* **72,** 5283 (1992).
22. P. M. Borsenberger, E. H. Magin, M. Van der Auweraer, and F. C. De Schryver, *Phys. Stat. Sol. (a)* **140,** 9 (1993).
23. P. M. Borsenberger and J. Shi, *Phys. Stat. Sol. (b)* **191,** 461 (1995).
24. P. M. Borsenberger and M. B. O'Regan, *Chem. Phys.* **200,** 257 (1995).
25. P. M. Borsenberger, *Jpn. J. Appl. Phys.* **35,** 2698 (1996).
26. P. M. Borsenberger, E. H. Magin, M. B. O'Regan, and J. A. Sinicropi, *J. Polymer Sci. B: Polymer Physics* **34,** 317 (1996).
27. P. M. Borsenberger, W. T. Gruenbaum, L. -B. Lin, and S. A. Viser, *SPIE Proc.* Vol. **3281,** 218 (1998).
28. Fredericq and C. Houssier, *Electric dichroism and electric birefringence,* Clarendon Press, Oxford, 1973.
29. H. Benoit, *Ann. Phys.* **6,** 561 (1951).
30. B. Kippelen, Sandalphon, K. Meerholz, and N. Peyghambarian, *Appl. Phys. Lett.* **68,** 1748 (1996).
31. P. G. Farrell and J. Newton *J. Phys. Chem.* **69,** 3506 (1965).
32. T. Sawyer, *Electrochemistry for chemists,* Wiley, New York, 1995, p. 203.
33. H. Reiss and A. Heller, *J. Phys. Chem.* **89,** 4207 (1985).
34. S. M. Silence, J. C. Scott, F. Hache, E. J. Ginsburg, J. K. Jenkner, R. D. Miller, R. J. Twieg, and W. E. Moerner, *J. Opt. Soc. Am. B* **10,** 2306 (1993).
35. R. Bittner, C. Bräuchle and K. Meerholz, *Appl. Opt.* **37,** 2843 (1998).